Hindawi
Advances in Mathematical Physics
Volume 2019, Article ID 8240587, 7 pages
https://doi.org/10.1155/2019/8240587

Research Article

Modelling of Nickel Atoms Interacting with Single-Walled Nanotubes

Mansoor H. Alshehri

Mathematics Department, College of Science, King Saud University, P.O. Box 2455, Riyadh 11451, Saudi Arabia

Correspondence should be addressed to Mansoor H. Alshehri; mhalshehri@ksu.edu.sa

Received 19 December 2018; Accepted 7 February 2019; Published 3 March 2019

Academic Editor: Nicola L. Rizzi

Herein, the encapsulation mechanism of nickel atoms into carbon and boron nitride nanotubes is investigated to determine the interaction energies between the nickel atom and a nanotube. Classical modelling procedures, together with the 6-12 Lennard-Jones potential function and the hybrid discrete-continuous approach, are used to calculate the interaction of a nickel atoms with (i, i) armchair and $(i, 0)$ zigzag single-walled nanotubes. Analytical expressions for the interaction energies are obtained to determine the optimal radii of the tubes to enclose the nickel atom by determining the radii that give the minimum interaction energies. We first investigate the suction energy of the nickel atom entering the nanotube. The atom is assumed to be placed on the axis and near an open end of a semi-infinite, single-walled nanotube. Moreover, the equilibrium offset positions of the nickel atoms are found with reference to the cross-section of the nanotubes. The results may further the understanding of the encapsulation of Ni atoms inside defective nanotubes. Furthermore, the results may also aid in the design of nanotube-based materials and increase the understanding of their nanomagnetic applications and potential uses in other areas of nanotechnology.

1. Introduction

The discovery of nanotubes such as carbon nanotubes (CNTs) and boron nitride nanotubes (BNNTs) has had an enormous impact on the study of many technological materials and nanomaterials [1–4]. CNTs comprise entirely carbon (C) atoms, while BNNTs contain an equal number of nitrogen (N) and boron (B) atoms. These nanotubes have a one-dimensional tubular structure. Their geometric configurations can be described by a chiral vector (i, j), where i and j are a pair of integers known as the chiral vector numbers [5–8]. The nanotube is called an armchair nanotube, when $i = j$, a zigzag nanotube, when $j = 0$, and a chiral nanotube, when $i \neq j$. CNT and BNNT structures can be single-walled or multiwalled [4, 5, 7, 8]. Owing to their geometries and attractive properties, such as resistance to oxidation, high absorption energies for some molecules, light weight, mechanical stiffness, and high electrical conductance, CNTs and BNNTs have attracted attention in the last two decades as promising materials for many potential applications including electrochemical actuation, field emission, and transistors [5, 9–13]. Although CNTs and BNNT have structural similarities, the electronic structures of BNNT are expected to be rather different from those of CNTs. For example, the distribution of charge is asymmetric in B-N bonds in BNNTs as compared to the C-C bonds in CNTs, which might create a significant difference between the two types of nanotubes [14]. The functionalization of molecular encapsulation inside nanotubes has given rise to a wide range of fundamental applications in areas of electronics, optics, biomechanics, thermodynamics, biochemistry, and magnetics [13]. The encapsulation of molecules inside nanotubes could be utilized to distinguish metallic CNTs from semiconducting CNTs and to increase CNT solubility in organic media [15]. Furthermore, one of the most important biomedical applications of nanotubes is their use as a delivery system for platinum drugs [16–18]. In addition, the combination of metal atoms and nanotubes is ideal for fabricating novel one-dimensional nanostructures with various arrangements, and filling nanotubes with magnetic elements like Ni can make them potentially applicable for the storage of magnetic data [19, 20]. Piskunov et al. [20] used first-principles calculations to investigate the encapsulation of nickel atoms into single-walled carbon nanotubes. They

found that the most preferable chiral vector numbers for Ni atom insertion into single-walled carbon nanotubes are (5,5) and (10,0). Yang et al. [21] investigated the interaction of Ni atoms with (5,5) armchair and (10,0) zigzag single-walled carbon nanotubes using density functional theory calculations. Their results showed that the energies for Ni binding to CNTs and the structures of CNTs are affected by the intrinsic defects which include double vacancies, single vacancies, and Stone-Wales defects. In addition, Zhang et al. [22] used first-principles calculations to investigate the adsorption and catalytic behaviour of nickel atoms inside (5,5), (6,6), and (7,7) BNNTs. They showed that Ni-BNNTs are promising low-temperature catalysts for CO oxidation. The encapsulation of various metal nanostructures inside CNTs and BNNTs has been successfully demonstrated by different groups using experiments and molecular dynamics simulations (see, for example, [20, 23–26]), but very few works in this field have used conventional applied mathematical modelling. Mathematical modelling, together with efforts of experimentalists and molecular dynamics (MD) simulations, can provide a deeper understanding of the interactions between molecules. In this paper, we consider nickel atoms encapsulated inside single-walled armchair (i, i) and zigzag $(i, 0)$ single-walled CNTs and BNNTs. We use the Lennard-Jones potential function together with the hybrid discrete-continuous approach to determine the optimal nanotube size to encapsulate Ni atoms.

2. Potential Energy

The van der Waals interaction energy between two atoms at a distance r apart is derived from the classical Lennard-Jones potential function $\Phi(r)$, which is given by

$$\Phi(r) = -\frac{A}{r^6} + \frac{B}{r^{12}}, \tag{1}$$

where A and B are the attractive and repulsive constants, respectively. The interaction energy between two nonbonded molecular structures can be obtained as a summation for each atomic pair, namely,

$$E = \sum_p \sum_q \Phi\left(r_{pq}\right), \tag{2}$$

where $\Phi(r_{pq})$ is a potential function for atoms p and q that are separated by a distance r_{pq} on two distinct molecular structures. Using the continuous approach (atoms are assumed to be uniformly distributed over the entire surfaces of the molecules), the double summation in (2) is replaced by the following double-surface integral for each molecule:

$$E = \eta_1 \eta_2 \int_{M_1} \int_{M_2} \Phi(r)\, dM_1\, dM_2, \tag{3}$$

where η_1 and η_2 are the mean atomic surface densities of the first and the second molecule, respectively, and r is the distance between the two typical surface elements dM_1 and dM_2. Note that the mean atomic surface density can be calculated by dividing the number of atoms which make up the molecule by the surface area of the molecule (i.e., η = number of the atoms/surface area of molecule). In this paper, we use the hybrid discrete-continuous approach to determine the interaction energy. The hybrid model, which is introduced by elements of both (2) and (3), is given by

$$E = \sum_k \eta \int \Phi(rk)\, dM, \tag{4}$$

where $\Phi(rk)$ is the potential function, η denotes the surface density of atoms on the molecule, which is considered continuous, and r is the distance between an atom k in the molecule, which is modelled as a summation over each of its atoms, and a typical surface element dM on the continuously modelled molecule. The values of the van der Waals diameters and well depths given in [27] are used here, and we note that these values have been widely used in many research areas. We find the attractive (A) and repulsive (B) constants for the interaction between different types of atoms m and n, as shown in Table 1, utilizing the van der Waals diameters σ and well-depths ε from Rappi et al. [27] for each atom type. We then used the empirical combining rules $\sigma_{mn} = (\sigma_m + \sigma_n)/2$ and $\varepsilon_{mn} = \sqrt{\varepsilon_m \varepsilon_n}$, where $A = 4\varepsilon\sigma^6$ and $B = 4\varepsilon\sigma^{12}$. In addition, the surface density of atoms on carbon and boron nitride nanotubes is assumed to be the same as those of their parent materials, namely, graphene and hexagonal boron nitride. The surface density of atoms on a sheet which comprises a tessellation of hexagonal rings can be easily calculated using the relation $\eta = 4\sqrt{3}/9\varrho^2$, where ϱ = 1.42 Å and ϱ = 1.45 Å for lengths of one carbon–carbon and boron–nitride bonds, respectively; thus the atomic surface densities of carbon and boron nitride nanotubes are η_c = 0.3821 Å^{-2} and η_{bn} = 0.3682 Å^{-2}, respectively. Moreover, the nanotube radii can be calculated from $a = \alpha\sqrt{i^2 + j^2 + ij}/2\pi$, where (i, j) denotes the chiral vector and $\alpha = \sqrt{3}\varrho$ Å.

Table 1: Numerical values of the attractive and repulsive constants.

Interaction	A (eV Å^6)	B (eV Å^{12})
C-Ni	4.797	3344.917
BN-Ni	10.7947	7666.393

3. Suction Energy of Ni Atom Entering Single-Walled Nanotube

In this section, we consider the energy of a nickel atom as it enters single-walled carbon and boron nitride nanotubes. In this case, the nanotube is assumed to be a semi-infinite cylinder without taking into account the effects of the other end and the cylinder length. Thus, we only need to consider the short range nature of the van der Waals forces. The Ni atom is assumed to have the coordinates $(0, 0, Z)$ and the nanotube of radius a is given parametrically by $(a\cos\phi, a\sin\phi, z)$, where $-\pi \le \phi \le \pi$ and $-\infty < z < \infty$, as shown in Figure 1. In this configuration, the distance r between the Ni atom and a typical point on the tube is given by

$$r^2 = a^2\cos^2\phi + a^2\sin^2\phi + (z - Z)^2 = a^2 + (z - Z)^2. \tag{5}$$

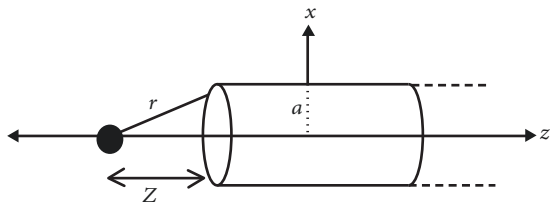

Figure 1: Schematic illustration of a Ni atom entering a single-walled nanotube.

Therefore, the total interaction energy of the Ni entering the tube is given by

$$E = a\eta_t \int_{-\pi}^{\pi}\int_{0}^{\infty}\left(-\frac{A}{r^6}+\frac{B}{r^{12}}\right)dz\,d\phi = a\eta_t\left(-AH_3+BH_6\right), \tag{6}$$

where η_t is the mean atomic surface density of the nanotube (CNT or BNNT). We evaluate the integral H_n $(n = 3, 6)$ as follows:

$$H_n = \int_{-\pi}^{\pi}\int_{0}^{\infty}\frac{1}{\left[a^2+(z-Z)^2\right]^n}dz\,d\phi. \tag{7}$$

The integral over ϕ is trivial, and therefore

$$H_n = 2\pi\int_{0}^{\infty}\frac{1}{\left[a^2+(z-Z)^2\right]^n}dz, \tag{8}$$

since the integrand is independent of ϕ. The integral H_n is evaluated over z by making the variable change $s = z - Z$, and we obtain

$$H_n = 2\pi\int_{-Z}^{\infty}\frac{1}{\left(a^2+s^2\right)^n}ds. \tag{9}$$

Upon making the substitution $s = a\tan\varphi$, the integral H_n becomes

$$H_n = 2\pi a^{1-2n}\int_{\chi}^{\pi/2}\sec^{2-2n}\varphi\,d\varphi = 2\pi a^{1-2n}\int_{\chi}^{\pi/2}\cos^{2n-2}\varphi\,d\varphi, \tag{10}$$

where $\chi = \tan^{-1}(-Z/a)$. The above integral can be evaluated using the formula from [28] ($\oint$ 2.512(2))

$$\int_{\chi}^{\pi/2}\cos^{2n-2}\varphi\,d\varphi = \left[\frac{\sin\varphi}{2n-2}\left(\cos^{(2n-3)}\varphi + \sum_{k=1}^{n-2}\left(\frac{(2n-3)(2n-5)\cdots(2n-2k-1)\cos^{2n-2k-3}\varphi}{2^k(n-2)(n-3)\cdots(n-1-k)}\right)+\frac{(2n-3)\varphi}{2^{n-1}(n-1)!}\right)\right]_{\chi}^{\pi/2}, \tag{11}$$

where $\sin\chi = -Z/(a^2+Z^2)^{-1/2}$ and thus $\cos\chi = a/(a^2+Z^2)^{-1/2}$. For the values of $n = 3$ and 6, the integral H_n can be expanded and evaluated to yield

$$H_3 = \pi a^{-5}\left[\frac{3\pi}{8}+\frac{3}{4}\tan^{-1}\left(\frac{Z}{a}\right)+\frac{3Za}{4\left(a^2+Z^2\right)}+\frac{Za^3}{2\left(a^2+Z^2\right)^2}\right] \tag{12}$$

and

$$H_6 = \pi a^{-11}\left[\frac{9\pi}{3840}+\frac{3}{640}\tan^{-1}\left(\frac{Z}{a}\right)+\frac{Za^9}{5\left(a^2+Z^2\right)^5}+\frac{9Za^7}{40\left(a^2+Z^2\right)^4}+\frac{7Za^5}{60\left(a^2+Z^2\right)^3}+\frac{Za^3}{16\left(a^2+Z^2\right)^2}+\frac{3Za}{80\left(a^2+Z^2\right)}\right]. \tag{13}$$

3.1. Results and Discussion. Using the aforementioned values of constants and the algebraic computer package MAPLE, the numerical solutions of the interaction energies of the Ni atom entering various carbon and boron nitride nanotubes are obtained. As shown in Figure 2, the results indicate that the Ni atom is accepted for all nanotubes with different radii, and the energies are more negative inside the tube (positive Z) than outside the tube (negative Z). Table 2 summarizes the results of the interaction energies between Ni atom and CNTs and BNNTs. Figure 2 and Table 2 show that the interaction energy is strongly dependent on the radius a of the nanotube. We observe that the nanotubes with radii bigger than $\approx$ 2 Å are accepted the Ni atom for both CNTs and BNNTs, and the values of interaction energy of Ni atom with nanotubes have been found increasing with radius of the nanotube growth. Also, by minimizing the energy, the results predict that the optimal of the values of the radius to enclose the Ni atom are 2.0344 Å and 2.072 Å for CNT and BNNT corresponding (3, 3) armchair nanotube and 2.741 Å and 2.790 Å for CNT and BNNT corresponding (7, 0) zigzag nanotube, respectively.

4. An Offset Ni Atom Inside a Single-Walled Nanotube

In this section, we study the interaction of the Ni atom situated inside a carbon and boron nitride nanotube. We calculate the potential energy of the interaction between the Ni atom and the nanotube, where the Ni atom is assumed to be located at a distance δ away from the tube axis. To determine the preferred position of a Ni atom inside a CNT or BNNT, Ni is assumed to be located at $(\delta, 0, 0)$ inside axially symmetric cylindrical polar coordinates of radius a, as shown in Figure 3, and the nanotubes are assumed to extend infinitely with coordinates $(a\cos\phi, a\sin\phi, z)$, where

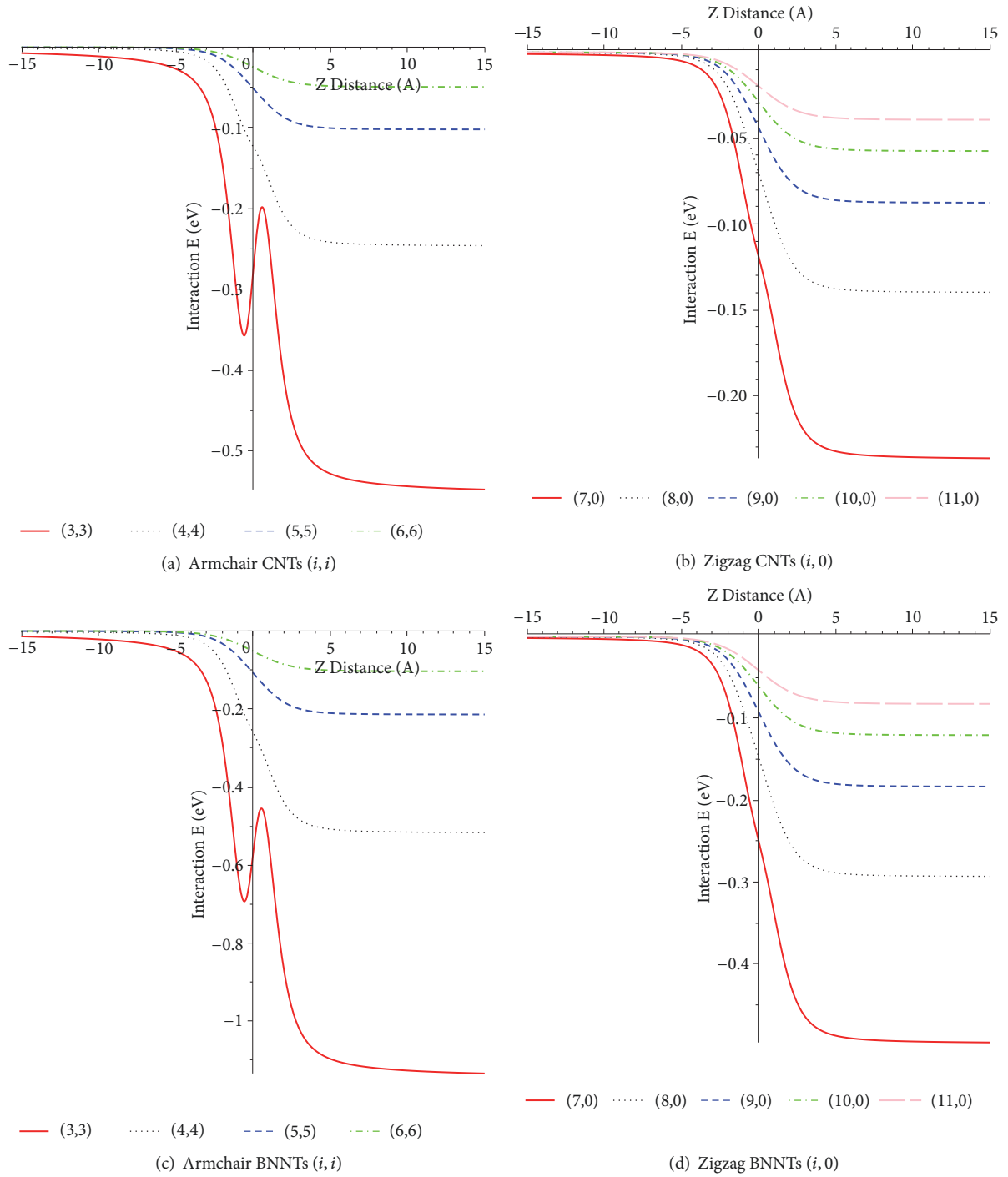

(a) Armchair CNTs (i, i)

(b) Zigzag CNTs $(i, 0)$

(c) Armchair BNNTs (i, i)

(d) Zigzag BNNTs $(i, 0)$

FIGURE 2: Typical interaction energies for a Ni atom entering nanotubes with different radii a.

$-\pi \le \phi \le \pi$ and $-\infty < z < \infty$. Thus, the distance r from the Ni atom to the wall of the nanotube is given by

$$\begin{aligned} r^2 &= a^2 - 2a\delta\cos\phi + \delta^2 + z^2 \\ &= (a-\delta)^2 + 4a\delta\sin^2\left(\frac{\phi}{2}\right) + z^2, \end{aligned} \tag{14}$$

and the total potential energy of the interaction of the Ni atom inside the nanotube is obtained by

$$\begin{aligned} E &= a\eta_t \int_{-\pi}^{\pi}\int_{-\infty}^{\infty}\left(-\frac{A}{r^6} + \frac{B}{r^{12}}\right)dz\,d\phi \\ &= \eta_t\left(-AK_3 + BK_6\right). \end{aligned} \tag{15}$$

Now, we evaluate the integral K_n $(n = 3, 6)$ as follows:

$$K_n = a\int_{-\pi}^{\pi}\int_{-\infty}^{\infty}\frac{1}{\left[(a-\delta)^2 + 4a\delta\sin^2(\phi/2) + z^2\right]^n}dz\,d\phi. \tag{16}$$

Table 2: Main results of the interaction of a Ni atom entering nanotubes.

Tube Type	Tube Radius (Å)		Interaction (eV)	
	CNT	BNNT	CNT/Ni	BNNT/Ni
(3,3)	2.0344	2.072	-0.554	-1.145
(4,4)	2.713	2.761	-0.246	-0.518
(5,5)	3.391	3.451	-0.102	-0.214
(6,6)	4.069	4.142	-0.049	-0.103
(7,0)	2.741	2.790	-0.237	-0.497
(8,0)	3.132	3.188	-0.139	-0.293
(9,0)	3.523	3.587	-0.087	-0.183
(10,0)	3.915	3.985	-0.057	-0.120
(11,0)	4.307	4.384	-0.039	-0.082

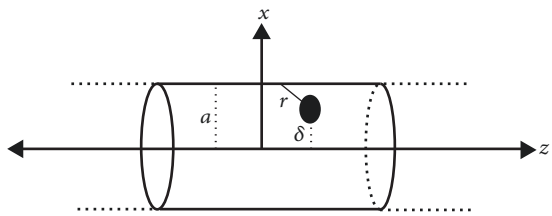

Figure 3: Schematic illustration of an offset Ni atom inside a single-walled nanotube.

We begin by defining $\omega^2 = (a-\delta)^2+4a\delta\sin^2(\phi/2)$ and making the substitution $z = \omega\tan\psi$, which gives

$$K_n = a\int_{-\pi/2}^{\pi/2}\cos^{2n-2}\psi\,d\psi\int_{-\pi}^{\pi}\frac{1}{\omega^{2n-1}}d\phi. \tag{17}$$

The first integral can be evaluated using the beta function, and thus K becomes

$$K_n = a\mathbf{B}\left(n-\frac{1}{2},\frac{1}{2}\right)\int_{-\pi}^{\pi}\frac{1}{\omega^{2n-1}}d\phi, \tag{18}$$

where $\mathbf{B}(p^*,q^*)$ denotes the beta function. To evaluate the second integral of K, the use of $\lambda = \sin^2(\phi/2)$ yields

$$K_n = \frac{2a}{(a-\delta)^{2n-1}}\mathbf{B}\left(n-\frac{1}{2},\frac{1}{2}\right) \times\int_0^1\lambda^{-1/2}(1-\lambda)^{-1/2}(1-\varpi\lambda)^{1/2-n}\,d\lambda, \tag{19}$$

where $\varpi = -4a\delta/(a-\delta)^2$. In the Euler form, the integral is given by

$$K_n = \frac{2\pi a}{(a-\delta)^{2n-1}}\mathbf{B}\left(n-\frac{1}{2},\frac{1}{2}\right) \times F\left(n-\frac{1}{2},\frac{1}{2};\frac{1}{2};1;\varpi\right), \tag{20}$$

where $F(a^*,b^*;c^*,z^*)$ denotes the usual hypergeometric function. Since $c^* = 2b^*$, we may use the quadratic transformation from [29], which gives

$$K_n = \frac{2\pi}{a^{2n-2}}\mathbf{B}\left(n-\frac{1}{2},\frac{1}{2}\right) \times F\left(n-\frac{1}{2},n-\frac{1}{2};\frac{1}{2};1;\frac{\delta^2}{a^2}\right). \tag{21}$$

4.1. Results and Discussion. By utilizing the aforementioned constant values together with the algebraic computer package MAPLE, we evaluated (15) to determine the preferred position of a Ni atom inside (5, 5), (6, 6), (10, 0), and (11, 0) carbon and boron nitride nanotubes. By minimizing the total potential energy of the Ni atom inside CNTs and BNNTs, Figure 4 shows that the preferred location of the Ni atom inside (5, 5) for both CNT and BNNT is on the tube axis (i.e., $\delta = 0$). In addition, for (6, 6), (10, 0), and (11, 0) nanotubes, we find that, for the case of CNT, $\delta = 0.952$ Å, $\delta = 0.756$ Å, and $\delta = 1.230$ Å, respectively. For the case of BNNT, $\delta = 1.001$ Å, $\delta = 0.804$ Å, and $\delta = 1.280$ Å, respectively. These results indicate that as the radius of the tube increases, the location where the minimum energy occurs tends to be closer to the nanotube wall.

5. Conclusions

This study investigated the interaction between nickel atoms and carbon and boron nitride nanotubes using the 6-12 Lennard-Jones potential function and the hybrid discrete-continuous approach to determine the preferred radii of the nanotubes for encapsulating the nickel atoms. We observed that the encapsulation of Ni atoms inside both CNTs and BNNTs depended strongly on the nanotube radius. In addition, we used the algebraic computer package MAPLE to numerically evaluate the interaction energies between a Ni atom and the nanotubes. The results indicated that the encapsulation of the Ni atom into a single-walled CNTs and BNNTs nanotubes may occur for nanotubes with greater than 2 Å. Our results are in a good agreement with others works [20, 22]. Moreover, these results indicate that the interaction between BNNTs and Ni atom is stronger than

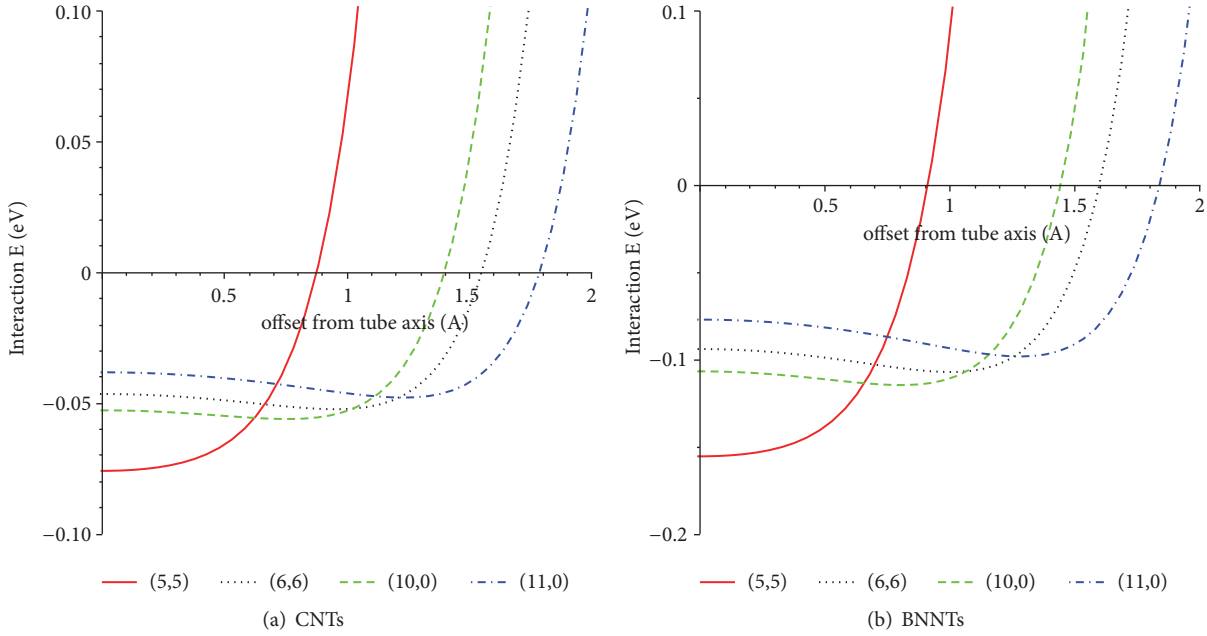

Figure 4: Total potential energy of an offset Ni atom inside CNTs and BNNTs with respect to the radial distance δ.

the interaction between CNTs and Ni atom since the former showed the lowest minimum energy. The results of this study may stimulate further studies of other metal atom interactions inside nanotubes.

Data Availability

No data have been used to support this study.

Conflicts of Interest

The author declares that they have no conflicts of interest.

Acknowledgments

This project was supported by King Saud University, Deanship of Scientific Research, College of Science Research Center.

References

[1] A. Rubio, J. L. Corkill, and M. L. Cohen, "Theory of graphitic boron nitride nanotubes," *Physical Review B*, vol. 49, no. 7, pp. 5081–5084, 1994.

[2] X. Blase, A. Rubio, S. G. Louie, and M. L. Cohen, "Stability and band gap constancy of boron-nitride nanotubes," *EPL*, vol. 28, pp. 335–340, 1994.

[3] S. Iijima and T. Ichihashi, "Single-shell carbon nanotubes of 1-nm diameter," *Nature*, vol. 363, pp. 603–605, 1993.

[4] S. Iijima, "Helical microtubules of graphitic carbon," *Nature*, vol. 354, pp. 56–58, 1991.

[5] M. S. Dresselhaus, G. Dresselhaus, and P. Avouris, *Carbon Nanotubes: Advanced Topics in the Synthesis, Structure, Properties and Applications*, vol. 80, Springer, Berlin, Germany, 2001.

[6] B. J. Cox and J. M. Hill, "Geometric polyhedral models for nanotubes comprising hexagonal lattices," *Journal of Computational and Applied Mathematics*, vol. 235, no. 13, pp. 3943–3952, 2011.

[7] C. Zhi, Y. Bando, C. Tang, and D. Golberg, "Boron nitride nanotubes," *Materials Science and Engineering R: Reports*, vol. 70, no. 3–6, pp. 92–111, 2010.

[8] A. Nigues, A. Siria, P. Vincent, P. Poncharal, and L. Bocquet, "Ultrahigh interlayer friction in multiwalled boron nitride nanotubes," *Nature Materials*, vol. 13, pp. 688–693, 2014.

[9] G. Mpourmpakis and G. E. Froudakis, "Why boron nitride nanotubes are preferable to carbon nanotubes for hydrogen storage?: an ab initio theoretical study," *Catalysis Today*, vol. 120, no. 3-4, pp. 341–345, 2007.

[10] Y. Chen, J. Zou, S. J. Campbell, and G. L. Caer, "Boron nitride nanotubes: pronounced resistance to oxidation," *Applied Physics Letters*, vol. 84, no. 13, pp. 2430–2432, 2004.

[11] M. Ishigami, S. Aloni, and A. Zettl, "Properties of boron nitride nanotubes," *AIP Conference Proceedings*, vol. 696, pp. 94–99, 2003.

[12] D. Hongjie, "Carbon nanotubes: synthesis, integration, and properties," *Accounts of Chemical Research*, vol. 35, Article ID 10351044, pp. 1035–1044, 2002.

[13] D. Cui, "Biomolecules functionalized carbon nanotubes and their applications," in *Medicinal Chemistry and Pharmacological Potential of Fullerenes and Carbon Nanotubes*, vol. 1 of *Carbon Materials: Chemistry and Physics*, pp. 181–221, Springer Netherlands, Dordrecht, Netherlands, 2008.

[14] M. L. Cohen and A. Zettl, "The physics of boron nitride nanotubes," *Physics Today*, vol. 63, no. 11, pp. 34–38, 2010.

[15] J. Li, J. Koehne, H. Chen et al., "Carbon nanotube nanoelectrode array for ultrasensitive DNA detection," *Nano Letters*, vol. 3, no. 5, pp. 597–602, 2003.

[16] H. Hillebrenner, F. Buyukserin, J. D. Stewart, and C. R. Martin, "Template synthesized nanotubes for biomedical delivery applications," *Nanomedicine*, vol. 1, no. 1, pp. 39–50, 2006.

[17] Z. Khatti and S. M. Hashemianzadeh, "Boron nitride nanotube as a delivery system for platinum drugs: drug encapsulation and diffusion coefficient prediction," *European Journal of Pharmaceutical Sciences*, vol. 88, pp. 291–297, 2016.

[18] C. R. Martin and P. Kohli, "The emerging field of nanotube biotechnology," *Nature Reviews Drug Discovery*, vol. 2, no. 1, pp. 29–37, 2003.

[19] P. Roy, S. Berger, and P. Schmuki, "TiO2 nanotubes: synthesis and applications," *Angewandte Chemie International Edition*, vol. 50, no. 13, pp. 2904–2939, 2011.

[20] S. Piskunov, J. Kazerovskis, Y. F. Zhukovskii, P. N. Dyachkov, and S. Bellucci, "Physics, chemistry and application of nanostructures," in *Proceedings of the International Conference Nanomeeting*, vol. 80, pp. 139–142, World Scientific Publishing Co. Pte. Ltd., Minsk, Belarus, 2013.

[21] S. H. Yang, W. H. Shin, J. W. Lee, S. Y. Kim, S. I. Woo, and J. K. Kang, "Interaction of a transition metal atom with intrinsic defects in single-walled carbon nanotubes," *Journal of Physical Chemistry B*, vol. 110, no. 28, pp. 13941–13946, 2006.

[22] Y. Zhang, Y. Liu, Z. Meng et al., "Confinement boosts CO oxidation on an Ni atom embedded inside boron nitride nanotubes," *Physical Chemistry Chemical Physics*, vol. 20, pp. 17599–17605, 2018.

[23] D. Golberg, F. Xu, and Y. Bando, "Filling boron nitride nanotubes with metals," *Applied Physics A*, vol. 76, pp. 479–485, 2003.

[24] C. Tang, Y. Bando, D. Golberg, X. Ding, and S. Qi, "Boron nitride nanotubes filled with Ni and $NiSi_2$ nanowires in situ," *Journal of Physical Chemistry B*, vol. 107, no. 27, pp. 6539–6543, 2003.

[25] T. Oku, N. Koi, I. Narita, K. Suganuma, and M. Nishijima, "Formation and atomic structures of boron nitride nanotubes with cup-stacked and Fe nanowire encapsulated structures," *Materials Transactions*, vol. 48, no. 4, pp. 722–729, 2007.

[26] L. Jin, X. Zhao, X. Qian, and M. Dong, "Nickel nanoparticles encapsulated in porous carbon and carbon nanotube hybrids from bimetallic metal-organic-frameworks for highly efficient adsorption of dyes," *Journal of Colloid and Interface Science*, vol. 509, pp. 245–253, 2018.

[27] A. K. Rappi, C. J. Casewit, K. S. Colwell, W. A. Goddard III, W. M. Skid, and J. Am, "UFF, a full periodic table force field for molecular mechanics and molecular dynamics simulations," *Journal of the American Chemical Society*, vol. 114, no. 25, pp. 10024–10035, 1992.

[28] I. S. Gradshteyn and I. M. Ryzhik, *Table of Integrals, Series and Products*, Academic Press, San Diego, Calif, USA, 6th edition, 2000.

[29] A. Erdelyi, W. Magnus, F. Oberhettinger, and F. G. Tricomi, *Higher Transcendental Functions*, vol. 1, McGraw-Hill, New York, NY, USA, 1953.